# Statistics of the Lagrangian Trajectories' Curvature in Thermal Counterflow

Naoto Sakaki[1*], Takumi Maruyama[†] and Yoshiyuki Tsuji[1†]

[1*]Graduate School of Engineering, Nagoya University, Furo-cho, Nagoya-city, 464-8603, Japan.

*Corresponding author(s). E-mail(s): sakaki.naoto@g.mbox.nagoya-u.ac.jp;
Contributing authors: c42406a@nucc.cc.nagoya-u.ac.jp;
[†]These authors contributed equally to this work.

**Abstract**

Small particle trajectories are visualized in thermal counterflow using the particle tracking velocimetry) technique, and the curvature of two dimensional Lagrangian trajectories of different particle size groups are studied in relation to acceleration and velocity. It is found that the PDF(probability density function) of curvature shows the same power-law tails independent of particle size, although the PDF of the vertical velocity depends on the particles size.

**Keywords:** PTV, thermal counterflow, curvature, helium4

## 1 Introduction

In recent years, visualization of thermal counterflow has been conducted by several researchers. particle tracking velocimetry(PTV) or particle image velocimetry are normally adopted for calculating the particle velocity. The solid hydrogen particles were used as tracer particles by Bewley *et al.* [1] and they visualized the quantum vortices. Paoletti *et al.* [2] reported probability density (PDF) of vertical velocity component in thermal counterflow, which has bimodal distribution but the horizontal component has a single peak. They are well approximated by Gaussian distribution. In addition, they observed that tracer particles can be trqpped by a quantum vortex and trajectory of particles

suddenly is bent when they are trapped. Guo *et al.* [3] conducted PTV measurement in thermal counterflow by using metastable helium molecules. Their study found that the normal fluid is in turbulent state at relatively large velocities. La Mantia *et al.* [4][5] pointed out that PDF of velocity and acceleration have a different shape depending on the length scale, $\ell_{\mathrm{exp}}$. It is the experimental probe length which is the distance between particles along the trajectories. For example, in the horizontal velocity in thermal counterflow, the shape of the PDF changes from unclassical power-law tails to classical Gaussian form as the length scale increases. In addition, the PDF tails of the horizontal acceleration, a, approaches to $a^{-5/3}$ scaling as length scales decrease. Kubo *et al.* [6] classified the particles into 4 groups and reported that the PDF of vertical velocity depends on the particle size.

As noted above, previous research on visualization of thermal counterflow mainly focused on the velocity and acceleration of tracer particles. But the curvature of tracer trajectories has not been studied in detail in regards to thermal counterflow. The curvature is importrant in the research of thermal counterflow as following reason. Whether the tracer particles are really trapped by the quntum vortices is questionable, because the difference of scale between the quantum vortex and the tracer partocle is 10000 times. Therefore, we need to understand the physics around the trapping, However, the detailed experimental analysis of the particle trapping has not been considered. The curvature can be usefull for the understanding of the trapping phenomenon since the trajectry of the tracer particle suddenly change around the trapping. That's why we need to study the curvature in thermal counterflow. In other words, it is sufficient to consider other physical quantities in the region where the curvature is high. Velocity can be candidate as the basic quantity, as has been seen in previous studies. Since the velocity distribution depends on the particle size [6], the curvature distribution may also depend on the particle size. Therefore, we need care when classifying. It is necessary to investigate the particle size dependence of the curvature as a preliminary step to classify the velocity conditioned by the curvature. Therefore, in this study, using the PTV technique, the motion of solid hydrogen particles in thermal counterflow is analyzed. In addition, we discuss the relation between the particle size and curvature of trajectories.

## 2 Experiments

The schematic representation of the experimental setup is shown in Fig. 1. The rectangular channel made of acrylic is set inside the cryostat [7]. The channel cross-section is $A = 20 \times 20$ mm$^2 m$ and the height is $H = 260$ m. The bath temperature varied from 1.9 to 2.1 K. The plate heater is located at the bottom, and the heat flux $q$ was 800 W/m$^2$. Datasets number of 1.9 [K], 2.0 [K], 2.1 [K] are 9, 17, and, 9, respectively for the robustness. The thermal counterflow is generated inside the channel. The experimental condition is listed in table 1. Bath temperature and heat current were in the range of

**Table 1** Experimental parameters of temperature $T$, heat current $q$, number of datasets, normal fluid velocity $v_n$, and superfluid velocity $v_s$.

| $T$ | $q$ | Number of datasets | $v_n$ | $v_s$ |
|---|---|---|---|---|
| 1.9 K | $\approx 800$ W/m$^2$ | 11 | 3.99 mm/s | $-2.88$ mm/s |
| 2.0 K | $\approx 800$ W/m$^2$ | 17 | 2.86 mm/s | $-3.53$ mm/s |
| 2.1 K | $\approx 800$ W/m$^2$ | 6 | 2.07 mm/s | $-5.91$ mm/s |

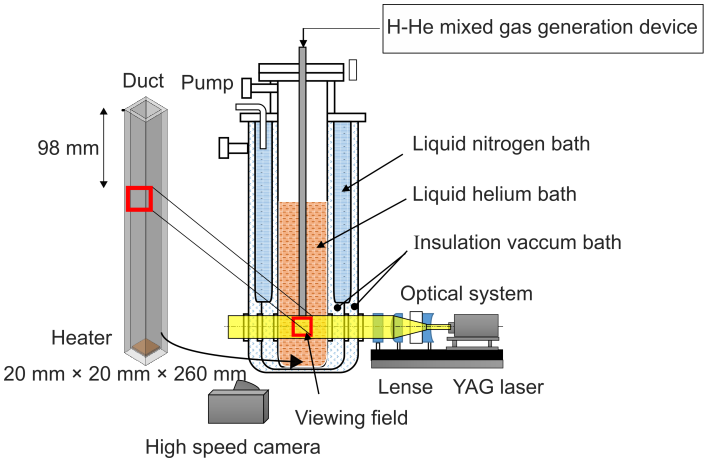


**Fig. 1** Schematic view of experimental settings.

experiments by Paoletti *et al.*[2]. A high-speed camera(1024×1024 pixels, 8 bit) was used for visualizing the area $8.7 \times 8.7$ mm$^2$ at 250 fps. A continuous laser (wavelength 532 nm, diode-pumped solid-state laser, and 4 W at maximum power) was adopted to make the laser sheet with a thickness of about 1 mm. A helium and hydrogen mixing chamber is designed to change the mixing ratio and the spouting pressure. The hydrogen particles were generated in the liquid helium. We adopted the condition of mixing ratio as He:$H_2$ = 40:1 and spouting pressure 20 kPa. The injection was done just above the $\lambda$ point, and then the bath temperature is decreased. In this study, the particle tracking algorithm developed by our group [7] is used. The size of the particle d is similar to that of the previous experiment [6], and it is about $3-20$ $\mu$m. In this research, we classify the size of particles in the same way as Kubo *et al.* [6].

## 3 Analysis method

In principle, the curbvature $\kappa$ is purely geometrical and contain no dynamical information about the trajectory. However, the curvature can be written in terms of the temporal derivatives along the trajectory. By Frenet formulas, the instantaneous curvature can be expressed as $\kappa = a_n u^{-2}$ [8], where $a_n$ is the magnitude of the normal acceleration and $u$ is the velocity as schematically shown in Fig. 2.

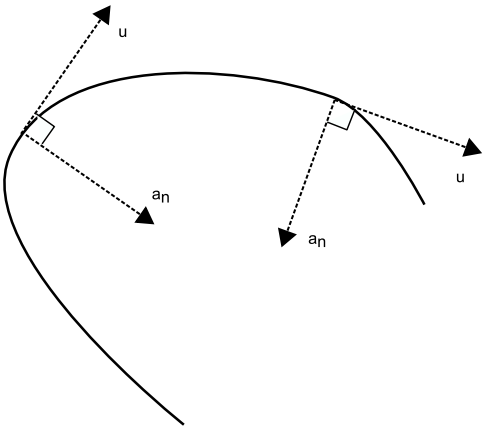


**Fig. 2** Example of particle trajectory (solid line), Lagrangian velocity and normal acceleration.

We use the PTV algorithm [9] to calculate the velocity and acceleration of the particles. Their velocity and acceleration were calculated by the numerical derivative with central difference method. The uncertainly is $O(\Delta t)$ for velocity and $O(\Delta t^2)$ for acceleration.

The distribution of $\kappa$ has been studied in classical turbulenc [8][10]. The PDF of $\kappa(P(\kappa))$ shows the two power-law regions where the high curvature region indicates $P(\kappa) \propto \kappa^{-5/2}$ and the lower one indicates $P(\kappa) \propto \kappa$. Xu *et al.* [10] reported that this feature can be understood by the Gaussian property of random variables but not by turbulent small-scale statistics. It is well known that the velocity fluctuation in classical turbulence is close to the Gaussian property. And, in addition, the velocity fluctuations $(ux, uy, uz)$ in homogeneous isotropic turbulence are independent of one another, then the magnitude $u^2 = u_x^2 + u_y^2 + u_z^2$ should follow a chi-squared distribution of degree of freedom 3. When $\kappa \to \infty$, or $\kappa \to 0$, the PDF of $\kappa$ follows the distribution of $u^{-2}$ with the assumption of finite an in this limit. And it indicates the power-law with exponent $-5/2$. In a similar way, the power-law scaling of $\kappa \to 0$ is derived. The PDF of curvature scales like the PDF of an as $a_n \to 0$ with the assumption that the components of an are independent Gaussian random variables. It is a reasonable approximation for small values of an, and the PDF of $a_n^2$ then follows a chi-squared distribution of degree of freedom 2 because the normal acceleration is confined to lie in the plane orthogonal to the velocity vector. In the case of $\kappa \to 0$, the PDF of $\kappa$ follows the distribution of $a_n$ as $a_n \to 0$. then the power-law with exponent 1 is derived [10]. The PDF of curvature in the two-dimensional case is similarly discussed. Since the PDF of an near 0 can be approximated as quasi Gaussian distribution, then, by using Taylor expansion, the power-law of PDFs are derived as $P(\kappa) \approx \kappa^{-2}$ and $P(\kappa) \approx \kappa^0$ in $\kappa \to \infty$ and $\kappa \to 0$, respectively. The PDF of curvature in two dimensions has been reported by Yang *et al.* [11]. They evaluated the distribution

of magnetic field line curvature by numerical simulation. We classified particles into 4 groups the same way as Kubo *et al.* [6]. By using particle size $d$, its average size $\alpha$ and its standard deviation $\sigma_p$, we divided the size of particles into four groups S($\alpha - 3\sigma_p \leq \ln d \leq \alpha - 0.67\sigma_p$), M($\alpha - 0.67\sigma_p \leq \ln d \leq \alpha$), L($\alpha \leq \ln d \leq \alpha + 0.67\sigma_p$), XL($\alpha + 0.67\sigma_p \leq \ln d \leq \alpha + 3\sigma_p$).

## 4 Resuls and Discussiton

Figure 3 show the PDF of the vertical velocity $v_y$ at bath temperature T = 2.0 K and heat flux $q$ = 780 W/m$^2$. The red circle represents XL size, the green square is L size, the blue asterisk is M size, and the black cross is S size. Velocity fluctuation is normalized by standard deviation $\sigma$. In table 2, parameters used in Fig 3 and Fig. 4 are listed. In other cases, the similar values are observed. Small size particles have a bimodal distribution but the large size particles(XL) have an unclear bimodal peak distribution. As reported by Kubo *et al.* [6], we confirmed that the PDF of vertical velocity depends on the particle size. In addition, in the case of T = 2.1 [K], the size dependency of vertical velocity PDF is less because the ratio of supefluid component is very small. Figure 4 is the PDF of curvature $\kappa$ for different sizes of particles. The symbol colors are the same as Fig. 3, but the graphs are shifted vertically not to overlap one another. $\sigma_u$ is the standard deviation of velocity and $\sigma_a$ is the standard deviation of acceleration. It is noted that PDF indicates the same power-law tails in high and low curvature regions independent of particle sizes. PDFs follow the power-law $\kappa^0$ and $\kappa^{-2}$ in low and high curvature regions, respectively. For the robustness, we calculate the exponent of the PDFs in all cases. These exponents are also observed in Fig. 5. Each exponents in low curvature region are caluclated in $10^{-3} < \kappa\sigma_u^2/\sigma_a < 3\times10^{-2}$. Each exponents in high curvature region are caluclated in $10^0 < \kappa\sigma_u^2/\sigma_a < 3\times10^1$. In Fig. 5, the symbol colors are the same as Fig. 3, but the dashed line represents 0 and the dashed dotted line represents 0. In addition, vertical errorbars represents the standard deviation of the exponents in each size group and temperature. These exponents are determined by the random Gaussian property of velocity and acceleration, but not by the small-scale turbulent intermittency effect. Detail discussions are referred to in the paper by Xu *et al.* [10]. Therefore, we may conclude that the curvature of small particle trajectories has similar PDF tails in both classical and quantum turbulence. Therefore, it could be suggested that the particle velocity components and normal acceleration are distributed like Gaussian in the limit of $\kappa \to \infty$ and $\kappa \to 0$. For future discussions, we analyze the statistical property of curvature and its relation to the vertical velocity.

**Table 2** Parameters used in Fig 3 and Fig. 4. Standard deviation of vertical velocity for each size, squared of standard deviation of velocity $\sigma_u^2$ for each size, standard deviation of acceleration $\sigma_s$ for each size, and sampling number for PDFs $N$ for each size,

| Size | $\sigma$ | $\sigma_u^2$ | $\sigma_a$ | $N$ |
|---|---|---|---|---|
| XL | 1.15 mm/s | 0.697 $mm^2/s^2$ | 145 $mm/s^2$ | 21179 |
| L | 1.22 mm/s | 0.697 $mm^2/s^2$ | 154 $mm/s^2$ | 7783 |
| M | 1.49 mm/s | 0.805 $mm^2/s^2$ | 296 $mm/s^2$ | 16057 |
| S | 2.07 mm/s | 2.58 $mm^2/s^2$ | 915 $mm/s^2$ | 13829 |

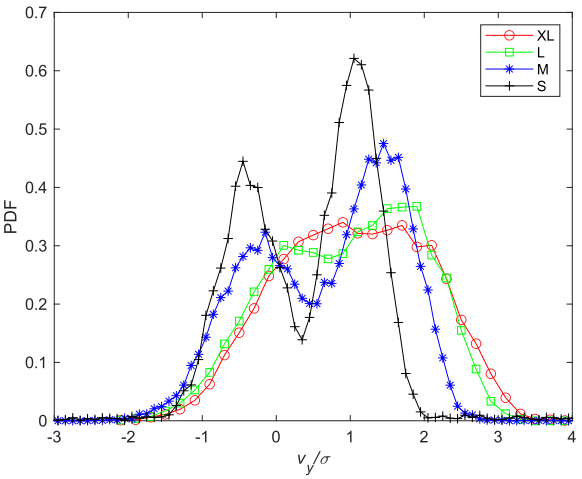


**Fig. 3** PDFs of the vertical velocity in each size group. Red circle is XL size, green circle is L size, blue circle is M size and black circle is S size.

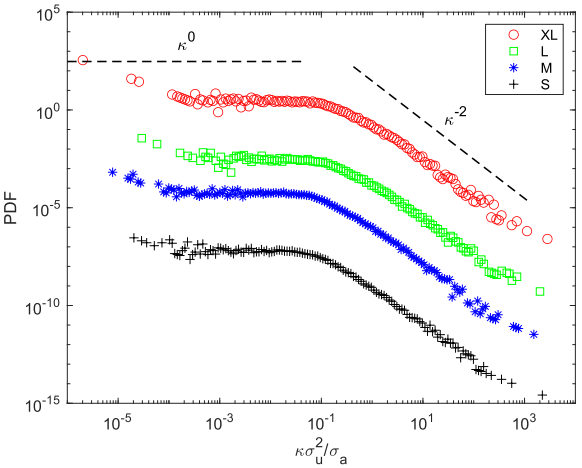


**Fig. 4** PDFs of the curvature in each size group. Red circle is XL size, green square is L size, blue asterisk is M size and black cross is S size. Plots are shifted vertically not to overlap each other.

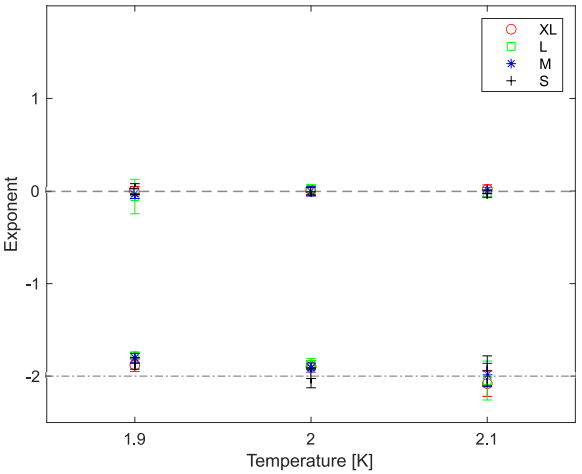


**Fig. 5** Exponents of the curvature in each size group and temperature. Red circle is XL size, green circle is L size, blue circle is M size and black circle is S size. Vertical errorbar represents the standard deviation of the exponents in each size group and temperature. The dashed line represents 0 and the dashed dotted line represents 0.

# 5 Conclusion

The curvature of two-dimensional Lagrangian trajectories in the thermal counterflow is calculated using the data measured by PTV. It is found that the PDF of curvature has two power-law tails. They are $\kappa^0$ and $\kappa^{-2}$ satisfied in low and high curvature regions, respectively. These features are confirmed indepen of particle sizes.

**Acknowledgments.** This work was supported by JSPS KAKENHI Grant Numbers JP19H00747, JP19H00641. The experimental support by Mr. S.Waki was indispensable in our measurements.

**Data Availability Statement.** Data are available on reasonable request.

# References

[1] G. P. Bewley, D. P. Lathrop and K. R. Sreenivasan, Visualization of quantized vortices, Nature, **441**, 588 (2006)

[2] M. S. Paoletti, R. B. Fiorito, K. R. Sreenivasan and D. P. Lathrop, Visualization of Superfluid Helium Flow, J. Phys. Soc. Jpn., **77**, 111007 (2008)

[3] W. Guo, S. B. Cahn, J. A. Nikkel, W. F. Vinen and D. N. Mckinsey, Visualization Study of Counterflow in Superfluid 4He using Metastable Helium Molecules, Phys. Rev. Lett, **105**, 045301 (2010)

[4] M. La. Mantia and L. Skrbek, Quantum or classical turbulence?, Europhys. Lett., **105**, 46002 (2014)

[5] M. La. Mantia and L. Skrbek, Quantum turbulence visualized by particle dynamics, Phys. Rev. B, 90, 014519 (2014)

[6] W. Kubo and Y. Tsuji, Statistical Properties of Small Particle Trajectories in a Fully Developed Turbulent State in He-II, J. Low Temp. Phys., **196**, 170 (2019)

[7] W. Kubo and Y. Tsuji, Lagrangian Trajectory of Small Particles in Superfluid He II, J. Low Temp. Phys., **187**, 611 (2017)

[8] W. Braun, F. De Lillo and B. Eckhardt, Geometry of particle paths in turbulent flows, J. Turbul., **7**, 1, (2006)

[9] We use particle tracking algorithm developed by John Crocker, Eric Weeks and David Grier.

[10] H. Xu, N. T. Ouellette and E. Bodenschatz, Curvature of Lagrangian Trajectories in Turbulence, Phys. Rev. Lett, **98**, 050201 (2007)

[11] Y. Yang, M. Wan, W. H. Matthaeus, Y. Shi, T. N. Parashar, Q. Lu and S. Chen, Role of magnetic field curvature in magnetohydrodynamic turbulence, Phys. Plasmas, **26**, 072306 (2019)